Neural Sensorless Control of Induction Motor

Emil Y. Marinov and Zhivko S. Zhekov(✉)

Department of Automation, Technical University of Varna,
Studentska Street 1, 9010 Varna, Bulgaria
e_marinov@tu-varna.bg, fitter@abv.bg

Abstract. In this paper are presented the problems for realization of direct adaptive neural sensorless control in combination with vector principle for induction motor control. Control system containing neural controllers of the speed and flux channels and neural speed estimator is proposed. These neural controllers perform a function of both speed and active stator current controllers (for the first channel), and respectively flux and excitation stator current controllers (for the second channel) compared to classical vector control. Neural speed estimator is designed as a neural model of the plant. For the controllers and estimator are used on-line trained backpropagation neural networks. Simulation research confirmed sufficient system performance at wide range input signal variation is done.

Keywords: Neural networks · Neural controller · Neural estimator · Sensorless vector control · Induction motor

1 Introduction

Vector controlled asynchronous electric drives are characterized with wide speed regulation range and high dynamic and static characteristics, but they are complex and nonlinear. That is why these systems are appropriate object for neural control [1–9]. In many cases using of speed sensor is undesirable due to rise of the cost, decrease of the reliability and technological limitations of the system. For that reason there is an increase interest to the sensorless electric drives where the information for the speed is recovered by estimator using measured motor currents and voltages [9–11].

In this paper are presented the opportunity for design of a sensorless asynchronous electric drive based on the two-channel structure of the control system with both neural control and neural estimation.

2 System Configuration

Generalized block diagram of the proposed system is shown in Fig. 1 where the abbreviations and variables are respectively: IM – induction motor; DM – driven machine; PM – power module; NE – neural estimator; BOVC – block for orientation and variables conversion; BC – block for compensation; NCS – neural controller of the speed channel; NCF – neural controller of the flux channel; ω_{ref} – reference angular

A. Abraham et al. (eds.), *Proceedings of the Second International Scientific Conference "Intelligent Information Technologies for Industry" (IITI'17)*, Advances in Intelligent Systems and Computing 679, DOI 10.1007/978-3-319-68321-8_42

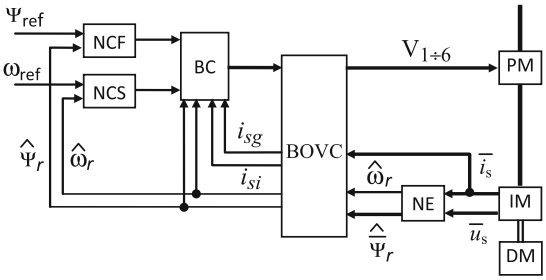

Fig. 1. Generalized block diagram of the system.

speed; $\hat{\omega}_r$ – estimated rotor speed, Ψ_{ref} – reference rotor flux; $\hat{\Psi}_r$ – estimated rotor flux, i_{si} – stator current active component; i_{sg} – stator current excitation component; $V_{1\div6}$ – PWM pulses.

Electromechanical processes in the IM and DM (for one-mass mechanical part) in stationary $\alpha\div\beta$ coordinate system are presented in complex form by Eq. (1).

$$\begin{aligned}
\bar{u}_s &= R_e(T_e p+1)\bar{i}_s - \frac{R_r L_m}{L_r^2}\bar{\Psi}_r + j\frac{L_m}{L_r}p_p\omega_r\bar{\Psi}_r \\
\bar{i}_s &= \frac{1}{L_m}(T_r p+1)\bar{\Psi}_r - j\frac{T_r}{L_m}p_p\omega_r\bar{\Psi}_r \\
M_e &= k_m\bar{\Psi}_r\bar{i}_s \\
M_e - M_c &= Jp\omega_r
\end{aligned} \tag{1}$$

where: $R_e = R_s + R_r\frac{L_m^2}{L_r^2}$; $L_e = \frac{L_s L_r - L_m^2}{L_r}$; $T_e = \frac{L_e}{R_e}$; $T_r = \frac{L_r}{R_r}$; $k_m = \frac{3p_p L_m}{2L_r}$; $p = \frac{d}{dt}$;
$\bar{u}_s, \bar{i}_s, \bar{\Psi}_r$ are representation vectors of the stator and rotor variables (voltage, current, flux); R_s, R_r – active stator and rotor resistances; L_s, L_r – total stator and rotor inductances; L_m – mutual inductance; p_p – pole pairs; M_e, M_c – electromechanical and load torques, J – moment of inertia.

PM contains uncontrolled rectifier and voltage inverter controlled by pulse width modulation (PWM). It is characterized with nonlinear and discrete features. BOVC is characterized with nonlinear features also.

The system contains two identical channels. The functional diagram of the one of them is shown in Fig. 2 where: P – plant containing IM, PM, BC, NE, BOVC; RM – reference model; NM – neural model of the plant; NC – neural controller; r – reference variable, u – control variable; y – output variable; $\hat{y}$ – estimated output variable; y_m – RM output variable.

For the channel of the speed mentioned above generalized variables are the first variables and for the channel of the rotor flux are the second variables in the brackets in Fig. 2; Δ^{-i}, Δ^{-j} – variables delays ($i = 1, 2, j = 0,1$, Δ^{-1} – delay with one sample). NM reproduces the plant behavior and it is learned so as to be minimized the error e_n. RM forms desirable behavior of the system – respectively desirable variation of the angular speed ω_m and rotor flux Ψ_m.

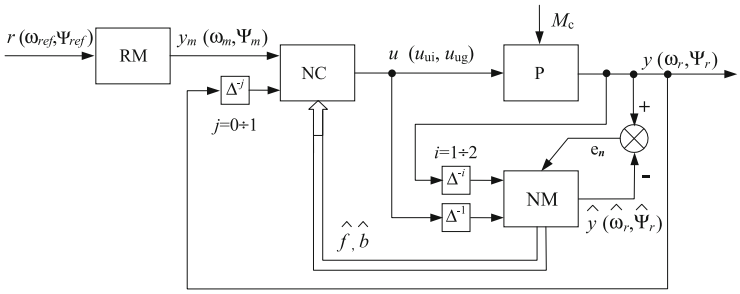

Fig. 2. Functional diagram of a system channel.

3 Neural Controller

Design of the controller is based on proposed in [7] modification of the method for design of a direct adaptive control presented in [1]. Assume that each of the plant channels are from the class nonlinear plants which are described with following discrete equation:

$$y(k+1) = f[y(k), y(k-1)] + bu(k) \tag{2}$$

where: f - unknown nonlinear function; b - unknown coefficient.

Assume that following equation describes the reference model:

$$\begin{aligned} y_m(k+1) &= a_{m1}y_m(k) + a_{m2}y_m(k-1) + b_{m1}r(k) + b_{m2}r(k-1) \\ &= f_m[y_m(k), y_m(k-1), r(k), r(k-1)], \end{aligned} \tag{3}$$

where: f_{m} - linear function.

Control signal is formed as:

$$u(k) = \{f_m[y_m(k), y_m(k-1), r(k), r(k-1)] - f[y(k), y(k-1)]\}/b. \tag{4}$$

It can be seen that calculation of the $u(k)$ is related with f and b finding.

For solving of this problem is used neural model of the plant. NM is described by:

$$\tilde{y}(k) = \hat{f}[y(k-1), y(k-2)]. \tag{5}$$

For purpose of NM simplifying, unlike [7], coefficient $\hat{b}$ (estimated value of b) is assumed to be constant and it is tuned once. Estimated output variable $\hat{y}(k)$ is calculated by:

$$\hat{y}(k) = \tilde{y}(k) + \hat{b}u(k-1) \tag{6}$$

The controller is based on the described NM at input signals translation with one sampling period ahead:

$$\tilde{y}(k+1) = \hat{f}[y(k), y(k-1)] \tag{7}$$

Assuming that:

$$\hat{f}[y(k), y(k-1)] \approx f[y(k), y(k-1)] \text{ and } \hat{b} \approx b \tag{8}$$

Equation (4) can be represented as:

$$\begin{aligned} u(k) &= \{f_m[y_m(k), y_m(k-1), r(k), r(k-1)] - \hat{f}[y(k), y(k-1)]\}/\hat{b} \\ &= [y_m(k+1) - \tilde{y}(k+1)]/\hat{b}. \end{aligned} \tag{9}$$

The output variable $y(k + 1)$ and the error $e(k + 1)$ are calculated respectively:

$$\begin{aligned} y(k+1) &= f[y(k), y(k-1)] - \tilde{y}(k-1) + \\ f_m[y_m(k), y_m(k-1), r(k), r(k-1)] &\approx y_m(k+1); \end{aligned} \tag{10}$$

$$e(k+1) = y_m(k+1) - y(k+1) \approx 0. \tag{11}$$

More accurately performing the assumption (8) leads to more accurately performing (10) and (11). The RM stability ensures the error convergence to zero.

Two identical neural models are used at solving of the reviewed task - the first model for the speed channel and the second model for the rotor flux channel. Two-layer backpropagation neural networks (NN) are used. Activation functions are respectively tansig and purelin for the first and second layer. The NN structure (the neurons number in each layer) is 5×1 and shown in Fig. 3, where: f_1 and f_2 are pointed above activation functions; w_1, b_1, w_2, b_2 – adjustable weights and biases; **p** – input vector.

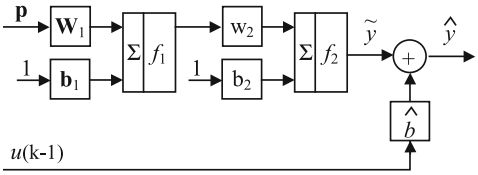

Fig. 3. Block diagram of the NM

Normalization of the input signals is made in the range $[-1 \div 1]$. The Levenberg-Marquart algorithm is used for NN training.

The input and target vectors for both channels are:

$$\begin{aligned} \mathbf{p}_{\omega}^{\mathrm{NM}}(k) &= [\omega(k-1), \omega(k-2)]'; \\ \mathbf{t}^{\mathrm{NM}}(k) &= \omega(k); \end{aligned} \tag{12}$$

$$\begin{aligned} \mathbf{p}_{\Psi}^{\mathrm{NM}}(k) &= [\Psi_2(k-1), \Psi_2(k-2)]'; \\ \mathbf{t}^{\mathrm{NM}}(k) &= \Psi_2(k). \end{aligned} \tag{13}$$

For neural controllers input vectors are respectively:

$$\mathbf{p}_{1\omega}^{\mathrm{NC}}(k) = [\omega(k), \omega(k-1)]' \tag{14}$$

$$\mathbf{p}_{1\Psi}^{\mathrm{NC}}(k) = [\Psi_2(k), \Psi_2(k-1)]' \tag{15}$$

Unlike [8], where are realized neural controllers of speed and flux only, the present article proposes neural controllers of the respective channels, i.e. these neural controllers performs a function of both speed and active stator current controllers (for the first channel), and respectively flux and excitation stator current controllers (for the second channel).

4 Neural Estimator

Neural estimator (NE) is designed as neural model of the plant. Neural network is trained on-line and approximates operating point of the IM [11].

NE block diagram is shown in Fig. 4 and contains two-layer backpropagation neural network. The first layer consists one neuron with one adjustable weight. Neurons in the second layer are two and their weights are non-adjustable. Estimated stator

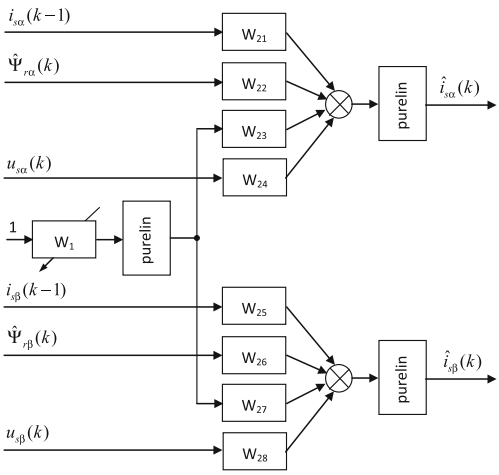

Fig. 4. Block diagram of the NE

current α and β components are formed on the output of each neuron in the second layer. NE is based on the induction motor discrete Eqs. (16) and (17):

$$\hat{i}_{s\alpha}(k) = (1 - T_0 T_e) i_{s\alpha}(k-1) + T_0 \frac{R_r L_m T_e}{L_r^2 R_e} \hat{\Psi}_{r\alpha}(k) + T_o \frac{L_m p_p T_e}{L_r R_e} \hat{\omega}'_r(k) \hat{\Psi}_{r\beta}(k) + T_0 \frac{T_e}{R_e} u_{s\alpha}(k); \quad (16)$$

$$\hat{i}_{s\beta}(k) = (1 - T_0 T_e) i_{s\beta}(k-1) + T_0 \frac{R_r L_m T_e}{L_r^2 R_e} \hat{\Psi}_{r\beta}(k) - T_o \frac{L_m p_p T_e}{L_r R_e} \hat{\omega}'_r(k) \hat{\Psi}_{r\alpha}(k) + T_0 \frac{T_e}{R_e} u_{s\beta}(k). \quad (17)$$

The estimated flux components $\hat{\Psi}_{r\alpha}$ and $\hat{\Psi}_{r\beta}$ are calculated by an Eq. (18), obtained from the Eq. (1) after excluding of the expression $p_p \omega_r \bar{\Psi}_r$.

$$\hat{\Psi}_{r\alpha} = \frac{L_r}{L_m} \frac{u_{s\alpha} - R_s i_{s\alpha}}{p} - \frac{L_s L_r - L_m^2}{L_m} i_{s\alpha}; \hat{\Psi}_{r\beta} = \frac{L_r}{L_m} \frac{u_{s\beta} - R_s i_{s\beta}}{p} - \frac{L_s L_r - L_m^2}{L_m} i_{s\beta} \quad (18)$$

The coefficients from these equations are NE weights:

$$w_1 = T_o \frac{L_m p_p T_e}{L_r R_e} \hat{\omega}'_r(k);$$

$$w_{21} = (1 - T_0 T_e); w_{22} = T_0 \frac{R_r L_m T_e}{L_r^2 R_e}; w_{23} = \hat{\Psi}_{r\beta}(k); w_{24} = T_0 \frac{T_e}{R_e}; \quad (19)$$

$$w_{25} = (1 - T_0 T_e); w_{26} = T_0 \frac{R_r L_m T_e}{L_r^2 R_e}; w_{27} = -\hat{\Psi}_{r\beta}(k); w_{28} = T_0 \frac{T_e}{R_e}.$$

The input and target vectors are respectively:

$$\mathbf{p}^{\mathrm{NE}} = \begin{bmatrix} i_{s\alpha}(k-1) \\ \hat{\Psi}_{r\alpha}(k) \\ u_{s\alpha}(k) \\ 1 \\ i_{s\beta}(k-1) \\ \hat{\Psi}_{r\beta}(k) \\ u_{s\beta}(k) \end{bmatrix}; \mathbf{t}^{\mathrm{NE}} = \begin{bmatrix} i_{s\alpha}(k) \\ i_{s\beta}(k) \end{bmatrix} \quad (20)$$

In the target vector are included actual stator current α and β components because on the NE outputs are derived estimated stator current α and β components. If $\hat{i}_{s\alpha}(k) \rightarrow i_{s\alpha}(k)$ and $\hat{i}_{s\beta}(k) \rightarrow i_{s\beta}(k)$ after training, then $\hat{\omega}_r \rightarrow \omega_r$.

The estimated speed is calculated by following equation:

$$\hat{\omega}_r(k) = w_1 L_r R_e / T_o L_m p_p T_e. \quad (21)$$

5 Simulation Research and Results

The research is conducted with induction motor AO 2 41-4. The motor rated power and current are respectively: 5.5 kW and 11.2 A. The load torque Mc is reactive and its range is $\pm M_n$ (M_n = 36.224 Nm – rated torque). In the plant simulation model are taken into account coordinate transformation and PM nonlinear and discrete properties.

Because approximately equal dynamics of the two channels of the system is used identical reference models with following coefficients: am1 = −1.9017, am2 = 0.9048, bm1 = $1.6120 \cdot 10^{-3}$, bm2 = $1.5592 \cdot 10^{-3}$. Sample time $T_0 = 10^{-5}$s.

The simulation results are shown in Figs. 5 and 6 where total moments of inertia are respectively $J = 1.5J_m$ and $J = 2.5J_m$ (J_m –moment of inertia of the motor).

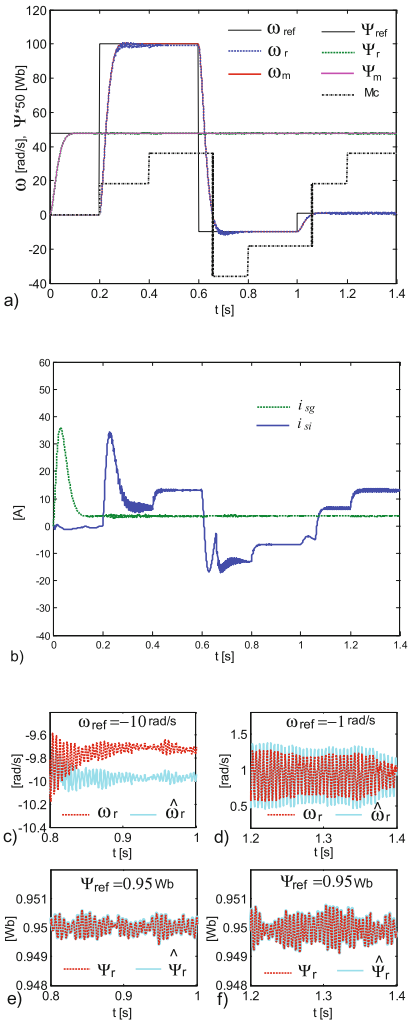

Fig. 5. System performance at $J = 1.5J_m$

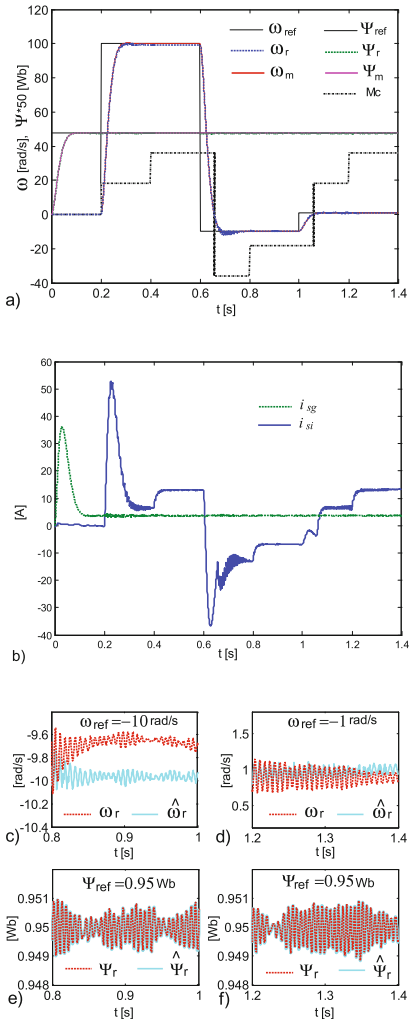

Fig. 6. System performance at $J = 2.5J_m$

Step variations are used for the reference speed ω_{ref} and load torque M_c. In all cases the system operates at initial excitation and constant rotor flux. In Figs. 5a and 6a are shown speed ω_r and rotor flux Ψ_r variation, their reference signals ω_{ref} and Ψ_{ref}, reference models variables ω_m and Ψ_m and load torque M_c. In Figs. 5b and 6b are shown respectively stator current active and excitation components. In Figs. 5cdef and 6cdef are illustrated more clear speed variation and its estimates, rotor flux variation and its estimates.

6 Conclusion

Neural adaptive sensorless vector control of an IM is proposed. The system is characterized by a simplified structure of the neural model for direct neural adaptive control realization, formed by two identical channels (speed and rotor flux) and neural speed estimator.

The simulation research confirms the system performance at reference speed, load torque and moment of inertia variations. The behavior of the system corresponds to the desired quality set by the reference model. The estimated speed and flux are dependent from active resistances variation, which would degrade the estimation accuracy and system performance as a result of an increase of a motor operating temperature.

Acknowledgements. This work was supported by the project НП-6, Research and synthesis of algorithms and systems for adaptive observation, control and filtration, Technical University of Varna.

References

1. Narendra, K., Mukhopadhyay, S.: Adaptive control using neural networks and approximate models. IEEE Trans. Neural Netw. **8**(3), 475–486 (1997)
2. Baruch, I., Cruz, I., Garrido, R., Nenkova, B.: An indirect adaptive vector control of the induction motor velocity using neural networks. Cybern. Inf. Technol. **7**(2), 57–72 (2007)
3. Vas, P.: Sensorless Vector and Direct Torque Control. Oxford University Press, Oxford (1998)
4. Cirrincione, M., et al.: Power Converters and AC Electrical Drives – With Linear Neural Networks. CRC Press, Boca Raton (2012)
5. Chan, T., Shi, K.: Applied Intelligent Control of Induction Motor Drives. John Wiley & Sons Ltd., Hoboken (2011)
6. Cristea, M., et al.: Neural and Fuzzy Logic Control of Drives and Power Systems. Newnes (2002)
7. Marinov, E.: Adaptive neural control of AC drive. Electrotechnica Electronica **9–10**, 62–67 (2006)
8. Kaminski, M., Orlowska-Kowalska T.: Adaptive neural speed control of the induction motor drive. Przeglad Elektrotechniczny, R. 89 NR 2a/2013, pp. 21–24 (2013). ISSN: 0033-2097
9. Bose, B.: Modern Power Electronics and AC Drives. Prentice Hall PTR, New Jersey (2001)
10. Holtz, J.: Sensorless control of induction motor. IEEE Trans. **90**(8), 1359–1394 (2002)
11. Zhekov, Z.: On-line neural speed estimator for sensorless vector control of induction motor. In: International Conference Automatics and Informatics 2010, Sofia, Bulgaria, vol. I, pp. 143–146 (2010)